International Journal of Applied Engineering Research ISSN 0973-4562 Volume 13, Number 11 (2018) pp. 9042-9052

AspenPlus™ model of stack cell reactor for the conversion of CO_2 and H_2S to CH_2O_2

[1]Jonathan C. Mbah[*], Rekisha A. Pootoon[2], Chengeto Kazuva[3]
Department of Chemical Engineering, Florida Institute of Technology, 150 University Blvd.,Melbourne, FL 32901-6975, USA
[*] Corresponding Author

Abstract

A 17.2 kW polymer electrode membrane electrolytic cell (PEMEC) stack is modeled for the conversion of CO_2 and H_2S feedstock to mainly formic acid (CH_2O_2) and elemental sulfur in AspenPlus™ simulation model V9 software. The cell operates at a moderate optimum pressure of 3 bar and at 120ºC, a temperature at which sulfur is a low viscous fluid and can flow out of the electrolytic cell without hindrance. The economics of this process rely heavily on power and electrolyzer stacks. When dealing with electrolysis, optimization of these two parameters is needed. To perform this optimization, we utilize the best configuration used in our material balance analysis: current density of 6.098 mA cm^{-2} at a cell potential of -1.238 V. The results indicate that there should be a balance between voltage and current density with respect to feed utilization and temperature should be operated at above 60% and above 100ºC values respectively. Temperature has significant impact on the current density as a result of increase in the cells kinetics. Thus, system efficiencies are expected to improve with temperature. However, this increase must be limited to temperatures at which sulfur is a low viscous fluid between 120 – 145ºC.

Keywords: AspenPlus simulation; CO_2; H_2S; CH_2O_2; Electrochemical; Current Density

INTRODUCTION

The continued emissions of greenhouse gas, such as carbon dioxide (CO_2), by human activities have been one of the greatest concerns in the effort to save our atmosphere for the future generations. Numerous studies have demonstrated that the emission of CO_2 offset the neutral carbon cycle already provided by nature. Notable CO_2 emission sources include fossil fuel based electric power plants, vehicles, manufacturing plants for cement, limestone, hydrogen, ammonia, and commercial and residential buildings [1]. The global rise in CO_2 emission requires multiple approaches to combat it such as switching from fossil fuel to more renewable energy sources, increasing the energy efficiency of buildings, increasing the fuel efficiency of vehicles, other sequestration approaches such as depletion of oil wells [2-4]. A recent approach to address this major challenge is the electrochemical reduction of CO_2 into useful chemicals such as reduction to carbon monoxide (CO), formic acid (CH_2O_2), methane (CH_4), and methanol [5, 6]. We have in this study modeled the feasibility of contacting CO_2 content feed gas from coal-fired flue gas with hydrogen sulfide (H_2S) gas, another potential pollutant which acts as a source of hydrogen, in an electrolytic cell to produce mainly CH_2O_2 and elemental sulfur using Aspen Technology design model V9 software. The simulation data for coal fired flue gas was obtained from the work of Xu et al.[7] which assumed that SO_2 and NOx materials including other impurities were removed using "molecular basket" adsorbent before being fed to the electroreactor.

There is considerable interest in focusing on using CO_2/formic acid. Formic acid is a safe, energy dense storage medium for hydrogen. Unlike more traditional fuels, like gasoline, CH_2O_2 is not flammable in 85% concentration, and is a commodity chemical, a raw material for a variety of products. Therefore developing technology to use CO_2 as a feedstock for CH_2O_2 production is very attractive. Similarly, petroleum refineries use hydrogen to improve the yields of more profitable products and to remove sulfur. The most common practice for the hydrogen supply is steam methane reforming of natural gas. A hydrogen sulfide waste stream from the hydrotreater process is partially oxidized to elemental sulfur and water by the Claus process. We have demonstrated the feasibility of extracting hydrogen proton electrolytically as a source of hydrogen, to be used for the CO_2 conversion, from the splitting of H_2S content feed gas due to its low Gibbs energy of formation [8]. Electrolytic splitting of hydrogen sulfide when combined with a flue gas stream containing CO_2 can yield sulfur and CH_2O_2, two useful chemicals.

The individual electrolyzer cell module measures 20 x 20 x 0.65 (225 cm^2 of active cell area) and consumes 1.72 kW. The stack system is composed of 10 single cells that consume ca. 17.2 kW in total. The cells are interconnected electrically to form a subsystem known as stack. During operation, the entire system is enclosed in a pressurized vessel at 3 bar to improve performance [9, 10].

ELECTROLYTIC SUBSYSTEM AND MODEL FLOWSHEET

A 17 kW GENEPAC fuel cell stack, developed by the French Atomic Energy Commission (CEA) was selected and modeled, however, this system has not been tested in a regenerative fuel cell mode using the current cell chemistry configuration that utilizes CO_2 and H_2S feed content gases. Multiple cells are interconnected in series in a vertical or bipolar plate stacking with sealing gasket around both sides to provide edge seals. Under compression, the edge gaskets create a gas-tight seal around each cell. In this configuration, a single conductive flow plate is in contact with both the feed electrode of one cell (the anode) and the feed electrode of the next (the cathode), connecting the two electrolytic cells in series. The plate serves as the anode in one cell and the

cathode in the next cell. Biplolar stacking is similar to how batteries are stacked on top of one another in a flashlight. This have the advantage of straightforward electrical connection between cells and exhibit extremely low ohmic loss due to the huge electrical contact area between cells. Thus this leads to electrolytic cell subsystem which are robust. Traditional PEM catalysts are unlikely for this application. Hence, our simulation is conducted with a composite polymer membrane (CPM) solid electrolyte of the type Nafion™ with added nano-scale hygroscopic oxide (silica) [11]. The nano-silica particles also play a role in water adsorption. The CPM experimental conditions of 393 K and 3 atm in the stack were used in the simulation as shown in Table 1. The mechanical properties of the CPM were enhanced by the presence of silica particles as evidenced by the high tensile strength value (1.6 N/cm^2) obtained for the CPM compared to 1.0 N/cm^2 obtained for bare Nafion™ membrane. When the water produced by electrochemical reaction at the cathode back-diffuses from cathode to anode, the silica, which has hygroscopic property, will adsorb the water. The water back-diffusion process also lends benefits by hydrating the membrane. As a result of the formation of strong absorption bonds between the water molecules and silica due to Van Der Waals forces, elevated temperatures cannot desorb the water adsorbed onto silica. The entire assembly called the polymer electrolyte membrane electrolytic cell (PEMEC) system is operated at elevated temperature and pressure. There are so many commercial and technological reasons to operate at these conditions. Rates of electrochemical kinetics are enhanced, sulfur is a low viscous fluid and can flow out easily, water management and cooling is simplified, and useful waste heat can be recovered. Below are the electrode reactions taken place in the PEMEC:

Anode compartment

$$2H_2S \rightarrow 2H^+ + 2e^- + 2S_{(l)} \quad (1)$$

Possible oxidation of H_2S by water was considered at the anode as given by the reaction:

$$2H_2S + H_2O \rightarrow SO_2 + 6H^+ + 6e^- \quad (2)$$

Cathode compartment

$$CO_2 + 2H^+ + 2e^- \rightarrow CH_2O_2 \quad (3)$$

$$H_2S + CO_2 \rightarrow CH_2O_2 + 1/8S_{8(l)}(2\ Faradays)@\Delta G = -10.908\ Kcal/mole\ @393\ K \quad (4)$$

Other reactions occurring at the cathode which were specified in the model are:

$$CO_2 + 3H_2O \rightarrow CH_3OH + H_2O\ @393\ K \quad (5)$$

$$CO_2 + 4H_2O \rightarrow CH_4 + 2H_2O\ @393\ K \quad (6)$$

$$2H^+ + 2e \rightarrow H_2\ @393\ K \quad (7)$$

$$2H^+ + 0.5O_2 + 2e \rightarrow H_2O@393\ K \quad (8)$$

$$CO_2 \rightarrow CO + 0.5O_2\ @393\ K \quad (9)$$

$$CO + H_2 \rightarrow CH_3OH@393\ K \quad (10)$$

Cell Overpotentials

Carbon dioxide electroreduction is known to present a variety of products from carbon monoxide to methane. Some conditions exist where formate ions can be selectively produced, the selectivity of reaction is highly dependent on some crucial parameters such as metal electrocatalyst, pH (the selectivity to formate anion being maximized when pH is close to neutrality), electrochemical potential, pressure, temperature. Conventional catalysts cannot achieve this selectivity. The role of catalysis is to level down the activation energy, to increase the kinetics of charge transfer and to orientate the CO_2 reduction to a specific product (in favorable conditions).

As a result, we considered only the cathode reaction kinetics because that is where significant cell polarization is experienced in most electrochemical cells. A composite cathode catalyst (M_1 = SnO_2 and M_2 =ZnTe), in which one constituent acts as the electron donor for the production of hydrogen radical while the other acts as a catalyst for the reduction of CO_2, was simulated based on experimental data that used electrodeposition method. This composite catalyst has been found based on our preliminary experiment to selectively form mainly formate anion. The preliminary experiment was conducted at 1.4 V using SnO_2/ZnTe cathode catalyst, the PEC cell delivered a current density of 5.12 mA cm^{-2} with a CH_2O_2 Faradaic efficiency of ~42%. The feed gas (CO_2 14%, H_2O 5.8%, O_2 5.0%, N_2 78%) was supplied by a portable gas analyzer BTU4500 Combustion Gas and Emissions analyzer from E Instruments. Note the experimental data did not include CO because of the detection limit of the analyzer used in the experiment. We used the literature data from the works of Xu et al. in order to include this gas in the simulation.

It was postulated that at the cathode, metal M_1 converts the migrated hydronium ion from the anode reaction to hydrogen with subsequent conversion to hydrogen radical. The hydrogen radical is adsorbed locally onto another metal (M_2) of known catalytic activity towards CO_2 hydrogenation. The advantage is that other intermediates formed will be reduced by the highly active hydrogen radical/metal hydride formed. Since the CO_2 partial pressure at the cathode is the dominant factor in determining the cathodic overvoltage, we can use the simplified form of the Butler-Volmer equation [10].

$$\eta_{cathode} = \frac{RT}{2\alpha F}\ln\left[\frac{j}{j_0 p^C\left\{y_{CO_2} \mid d - t^C jRT/\left(2Fp^C D^{eff}_{CO_2,N_2}\right)\right\}}\right] \quad (11)$$

where p^C is the total pressure at the cathode and y_{CO2} is the carbon dioxide mole fraction at the cathode catalyst layer, α is the transfer coefficient, $D^{eff}_{CO_2,N_2}(cm^2/s)$ is effective CO_2 diffusivity. The apparent CO_2 diffusivity is from the work of Ren et al. at transient and steady state CO_2 permeate data using a time-lag method derived from the Fick's second law of diffusion under 75% relative humidity in Nafion membrane [12]. The effective H_2S diffusivity,

$D^{eff}_{H_2S,H_2O}(1.27\times10^{-7}\,cm^2\,s^{-1})$ at the anode is not significant and can be neglected in addition to the low permeability of H_2S in Nafion. Note that we use atm as the unit of pressure p and the reference pressure p_0, which is 1 atm, disappears. However, since there is no N_2 diffusion flux in the electrolytic cell (no generation or consumption of N_2), we will simply ignore the nitrogen flux.

The ohmic overvoltage due to the membrane resistance in the PEMEC is approximated by the following equation:

$$\eta_{ohmic} = j \times ASR_m \tag{12}$$

where ASR_m is the area specific resistance, R_m is the total resistance of the membrane. Since the conductivity of the Nafion can change locally depending on water content, the total resistance of the membrane is found by integrating the local resistance over the membrane thickness (t_m) as

$$R_m = \int_0^{t_m} \frac{dz}{\sigma[\lambda(z)]} \tag{13}$$

where σ is the ionic conductivity of charged species and λ is the water content of Nafion. The σ increases linearly with increasing water content and exponentially with increasing temperature [9].

The Nernst potential established by gaseous oxidant and reductant is giving by the partial pressures of these gaseous substance as

$$\eta_{Nernst} = (RT/2F)\ln[p_{CH2O2}/p_{H_2S}p_{CO_2}] \tag{14}$$

Finally, the overall electrode potential including the reversible potential, V_{thermo}, is

$$V = \eta_{thermo} + \eta_{ohmic} + \eta_{cathodic} + \eta_{Nernst} \tag{15}$$

A design spec block '*DS-1*' was used to manipulate the required cell operating voltage by setting the input '*EMF-VCELL'=0* where '*EMF*' is the input voltage and '*VCELL*' is the calculated voltage. This voltage was sufficient to drive the power input to obtain the corresponding current generated by the electrode reaction.

Stoichiometric Number

It is common to operate an electrolytic cell at a certain stoichiometric number to maximize electrolytic cell efficiency. The stoichiometric number λ reflects the rate at which a reactant is provided to an electrolytic cell relative to the rate at which it is consumed. For example, λ = 2 means that twice as much reactant as needed is being provided to the electrolytic cell. Choosing an optimal λ is a sensitive task. A large λ is wasteful, resulting in parasitic power consumption and/or lost fuel, while small value, however, results in reactant depletion. Obviously, two stoichiometric number must be provided to in the cell – one for CO_2 and one for H_2S. We can define the stoichiometric number based on the ratio of the inlet to consumption fluxes:

$$\lambda_{H_2S} = \frac{J_{H_2S,\,inlet}}{J^A_{H_2S}} \qquad \lambda_{CO_2} = \frac{J_{CO_2,\,inlet}}{J^A_{CO_2}} \tag{16}$$

AspenPlus™ simulation

The thermal conductivity is like electrical conductivity, determined largely by the free electrons. Both thermal and electrical conductivity depend in the same way on not just the mean free path, but also on other properties such as electron mass and even the number of free electrons per unit volume. The ratio of thermal to electrical conductivity depends primarily on the square of the thermal speed [13]. But this square is proportional to the temperature, with the result that the ratio depends on temperature, T, and two physical constants: Boltzmann's constant, k, and the electron charge, e. Boltzmann's constant is, in this context, a measure of how much kinetic energy an electron has per degree of temperature.

A design model implemented in our simulation of the electrolytic cell is similar to that applied in a silicon transistor where silicon component is bolted to the metal frame of a piece of equipment [14-16]. In our case, a model heat flow from the electrolyte-catalyst junction can be constructed. The heat has to flow from the junction to the metalwork. The metalwork will conduct heat fast enough to keep temperature less than the ambient air. An important parameter will be the power consumption required by the cell before it overheats. The heat generated (exothermic reactions) and consumed (endothermic reactions) by other electrochemical reactions in the cell cathode and anode respectively, will balance each other thereby maintaining the temperature of the entire cell.

Consider the cell components, the electrolyte and the catalyst layers, are bolted to the encased electron conducting frame that constitutes the cell. The calculations are as follows.

$$Q_{MAX} = \frac{T_{JMAX} - (T_{AMB} + \Delta T_{HS})}{R_{\theta JC} + R_{\theta B} + R_{\theta EA}} \tag{17}$$

where Q_{MAX} (W) is the maximum power the cell can supply to limit the temperature of the cell to a safe level, T_{JMAX} (ºC) is the maximum junction temperature between the electrolyte and the catalyst layer, T_{AMB} is the ambient air temperature, ΔT_{HS} is the temperature difference above the ambient, $R_{\theta JC} + R_{\theta B}$ (ºC/W) are the total absolute thermal resistance from cell to ambient, $R_{\theta EA}$ is the absolute thermal electrolyte resistance [17]. Note however, the electrical and thermal differential equations are analogous, the analogy between electrical and thermal resistance in terms of practical basis is yet to be established. This is because a material that is considered an insulator in electrical terms is about 20 orders of magnitude less conductive than a material that is considered a conductor, while, in thermal terms, the difference between an "insulator" and a "conductor" is only about three orders of magnitude [18, 19]. The entire range of thermal conductivity is then equivalent to the difference in electrical

conductivity of high-doped and low-doped catalytic membrane.

The block used here to model the electrolytic cell in AspenPlus™ is the '*RGIBBS*'. This block is desirable in cases where information on the stoichiometry is unknown and, especially, if phase changes accompany the reaction an approach based on minimizing the Gibbs free energy of the whole mixture [20, 21]. In this approach, the total Gibbs energy of all components (reactants, products, and inert) is minimized. It is an ideal reactor where the reactions taken place in the reactor are not known or where there are multiple products involved as a result of reactions occurring inside of the reactor. However, this block model reactor requires accurate thermodynamics since Gibbs energy is calculated from enthalpy and entropy. Based on the operating conditions inside our electrolytic reactor (3 bar, 120°C), an ideal property method is best suited for our simulation model.

Three block were used to model one electrolytic cell. The anode '*RGIBANOD*' and the cathode '*RGIBCATOD*' are separated by a '*SEP*' block that separate the liquid sulfur and the hydrogen proton H^+. The H^+ is the charge carrier in a PEMEC. Due to the low Gibbs free energy of formation of H_2S, it easily split into elemental sulfur and H^+ at the anode at a temperature at which sulfur is a low viscous fluid and can easily flow out of the electrolytic cell. The H^+ is transported through the electrolyte to the cathode side where it reacts with CO_2 and electrons e^- to produce CH_2O_2. This cannot be modelled in Aspen Plus; therefore the overall reaction (3) was used in the simulation. Reactions (3) through (9) were specified in the '*RGIBCATOD*' block and it was assumed that they reach equilibrium at the operating temperature (*Top* = 393°C).

Table 1: Physical properties of PEMEC used in the AspenPlus™ simulation

Thermodynamic voltage, V_{thermo} (V)	0.24
Operating current density, j ($A\ cm^{-2}$)	6.098
Temperature, *T (K)*	393
Vapor saturation pressure, p_{SAT} (atm)	0.307
Hydrogen mole fraction, y_{H2}	0.422
Carbon dioxide mole fraction, y_{CO2}	0.952
Anode H_2S mole fraction, y_{H2S}	0.8
Anode H_2O mole fraction, y_{H2O}	0.2
Cathode H_2O mole fraction, y_{H2O}	0.003
Cathode pressure, p^C (atm)	3.0
Anode pressure, p^C (atm)	3.0
Effective hydrogen diffusivity, $D^{eff}_{H_2,H_2O}(cm^2\ s^{-1})$	0.149 [9]
Effective CO_2 diffusivity, $D^{eff}_{CO_2,H_2O}(cm^2\ s^{-1})$	4.15 x 10^{-6} [22]
Water diffusivity in Nafion, D_λ ($cm^2\ s^{-1}$)	3.81 x 10^{-6} [9]
Transfer coefficient, α	0.5 [10]
Exchange current density, j_0 ($A\ cm^{-2}$)	0.0001 [9]
Electrolyte thickness, t^M (μm)	125 [9]
Anode thickness, t^A (μm)	350 [9]
Cathode thickness, t^A (μm)	350 [9]
Gas constant, R (J mol^{-1} K^{-1})	8.314
Faraday constant, F (C mol^{-1})	96,485
Overall fuel utilization	85%
Active area of cell, (cm^2)	2,250 (10 cells)
Coal fired flue gas feed composition	CO_2 12.8%, CO 50 ppm, H_2O 6.2%, O_2 4.4%,N_2 76.6% [7]
Hydrogen sulfide composition	H_2S 90%, H_2O 10% [23]
PEMEC thermal loses, (kW)	0.09
Stoichiometric number	1.05

The stream '*VFLUEIN*' is fed to '*COM-C*', the flue gas compressor and its discharge pressure was set to about thrice the '*RGIBCATOD*' pressure to be able to drive the recycled stream from '*FSPLIT*'. The conventional pressure limitation for Nafion membrane is about 4 atm and at this pressure the boiling point of water is reported to be 145°C [24]

The flue gas composition and thermodynamic condition are inputted and the molar flow rate of fresh feed entering both the anode and the cathode were set by the '*FORTRAN CALCULATOR*' block in AspenPlus™ V.9 simulation package [25].

Fresh H_2S '*VH_2SIN*' stream and recycled stream '*SA9*' from the anode chamber are mixed in the block called '*EJECTORA*' and fed to the anode compartment where it contacts the catalytic anode and hydrogen proton selective membrane in the block called '*RGIBANOD*'. The H_2S then split into H^+, electrons and elemental sulfur. The sulfur flows out of the anode chamber as a low viscosity fluid at temperature of operation (120°C). The solid membrane is impermeable to the electrons which are then forced through the hypothetical external circuit as a heat duty (*QH2*) via the electrode. The H^+ migrate through the solid membrane as H_3O^+, and at the catalytic cathode combines with the electrons and fresh flue gas '*VFLUEIN*' feed that was mixed with unreacted CO_2 '*SC9*' from the block called '*EJECTORC*' to form CH_2O_2. The slightly exothermic reaction at the anode and the release of electrons forms the heat duty, *QH2*, and coupled with the transported H^+ complete the electrode reaction at the cathode. The overall Gibbs energy, ΔG, of the process is (-10.908 kcal/mole), with a net energy of about 0.24V per mole, as shown in Eqn. 1, because of the favorable thermodynamics provided by the low Gibbs free energy of H_2S formation.

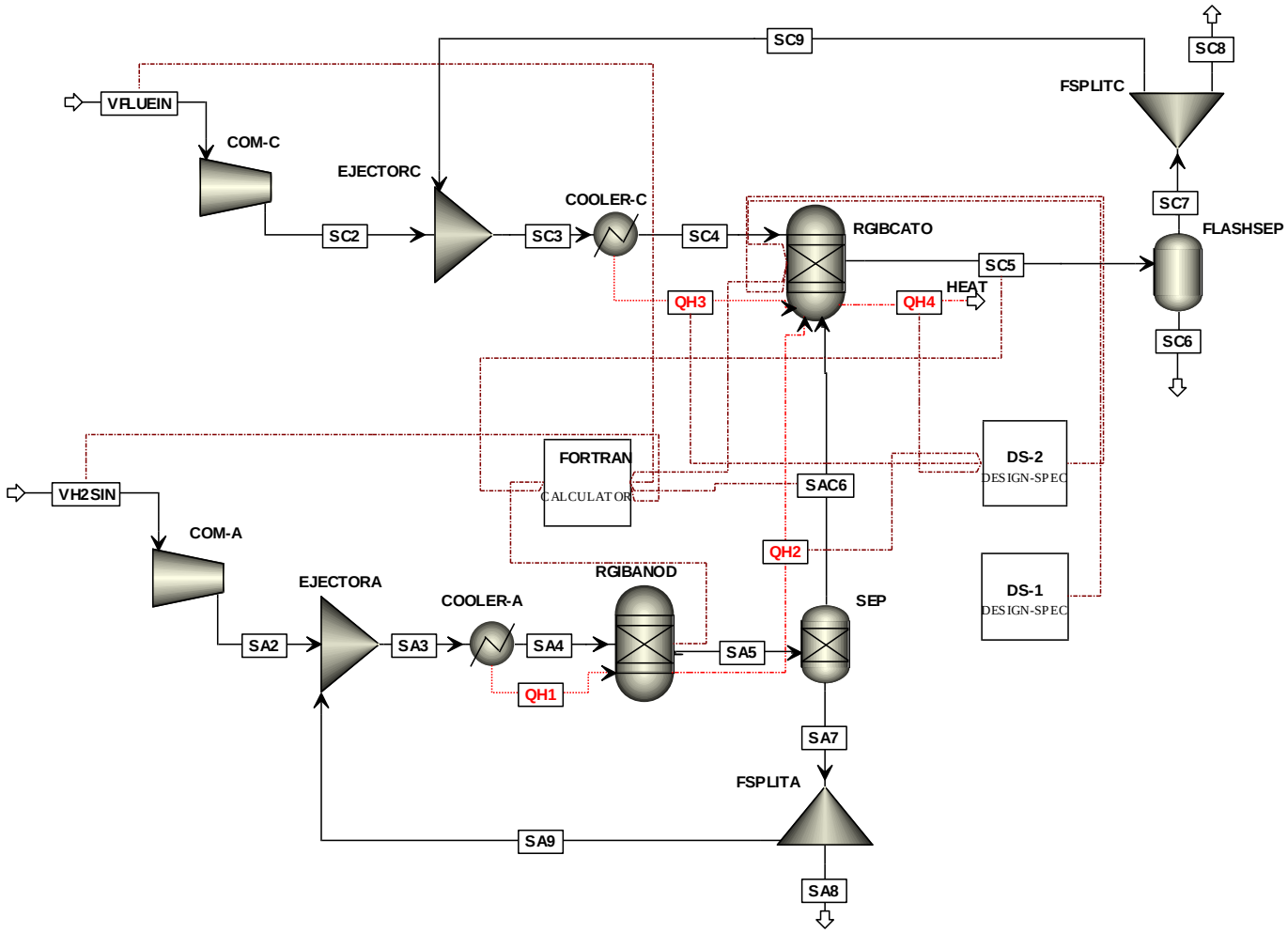

Figure. 1. Model flowsheet used in the AspenPlus™ simulation showing *FORTRAN* calculator and design spec blocks and their flow streams.

The fresh H_2S (*VH_2SIN*) and water vapor stream is fed to the anode side at elevated temperature 110°C in order to maintain the desired relative humidity in the cell at the cell operating pressure, 3 bar. The high relative humidity will ensure the Nafion composite membrane remains hydrated for it to transport the H^+ effectively. Stream '*SA4*' enters the '*RGIBANOD*' block, whose function is to separate out the H^+ required for the electrochemical reaction (*VH_2*, consumed).

Another design spec block '*DS-2*' in AspenPlus™ is used to set the electrolytic cell reactor at adiabatic condition and also to maintain the temperature of the system at 120°C. This is achieved by specifying that the heat streams ('*QH2*' + '*QH2*') – '*QH4*'=0, while the heat streams '*QH1*' and '*QH3*' were used to maintain constant temperature in the system through the blocks '*COOLERA*' and '*COOLERC*' respectively.

Furthermore, the '*FORTRAN CALCULATOR*' block in Aspen Plus is used extensively to simulate the electrochemical reactions taken place in the anode and the cathode blocks, including the control of fresh feed streams through manipulation of input parameters as described next. The chosen model takes the input temperature and cell resistances to calculate the corresponding power as given in Eq. 17, and the required voltage is calculated from Eq.15. These calculated power and voltage were then used to compute the current generated from the electrode reactions taken place in the cell. For calculated current (*I*), the calculator block sets the input H_2 equivalent flow using: *VH2EQ=N*(0.018655*CURRENT*3600)/(1000*U*$_{FUEL}$*)*. Thereafter, the fresh H_2S feed and the CO_2 feed are respectively calculated *VH2SIN=1.5*VH2EQ* and *VCO2IN=VH2EQ*U*$_{FEED}$ where *N* is the total number of cells required to achieve the given current and the value 1.05 is the stoichiometric number. The block H_2 split fraction, '*FSPLITA*' is set using the following equations: U_{FEED} =*VH2*, consumed/*VH2EQ*, where *VH2*, consumed is calculated. The required *VCO2* consumed at the 'R*GIBCATO*'= *VH2EQ* (from Eqn.4), and CO_2 split fraction, '*FSPLITC*' = *VCO2,* consumed/*VCO2IN*, which is equivalent to CO_2 utilization, U_{CO2}. The feed utilization factor (U_{FUEL}) and '*VH2EQ*' are known. The two recycled streams '*SA9*' and '*SC9*' exiting the anode and the cathode split blocks are fed to the ejector blocks '*EJECTORA*' and '*EJECTORC*' respectively to combine with fresh H_2S and flue gas streams. The gross and faradaic efficiencies are determined next. The gross efficiency is defined as: η*el,gross = Pelec,AC*/(*VH2SIN*LHVfuel*) where *Pelec,* is the total AC power (kW) requirement, *VH2SIN* is the molar flow rate of input fresh H_2S feed (kmol/s) and *LHVfuel* is the lower heating value of the input H_2 (*LHVfuel* =119.96 MJ kg^{-1} H_2). The faradaic efficiency is defined as: ηH_2S, = *VH2EQ/VH2SIN*.

Energy Balance Calculation

The unused power input to the cell generates heat together with the reaction heats from the electrode reactions at the anode and the cathode which are lost heat if the temperature of the cell is to be kept isothermally. Some of the heat is used in the inlet fuel streams at the anode and the cathode, but a significant part of the heat is used by some endothermic reactions occurring at the cathode even though the net heat output at the cathode is exothermic. To maintain the cell operating temperature at a stable point, two coolers are installed at both cell compartment to cool the stack. Since AspenPlus™ performs block net heat duty calculations [10], for the '*RGIBANOD*' and '*RGIBCATOD*' block model, the net heat duty '*QH4*' is calculated as

$$QH_4 = Q_{r1} + Q_{r2} + Q_{r3} + Q_{r4} + Q_{r5} + Q_{r6} + Q_{r7} + Q_{r8} + Q_{r9} + Q_{r10} - Q_{COMP} \quad (18)$$

where Qr1-10 are the heat of reactions at the anode and the cathode given by Eqns. 1-10, and Q_{COMP} were the heat given to the feed streams by compressors '*COM-A*' and '*COM-C*'. It is realistic to assume that certain amount of heat losses occurred at the two coolers '*COOLERA*' and '*COOLERC*' as 'Q_{losses}' (see Table 1). Hence the overall energy balance to keep the system operating isothermally is

$$QH_4 - Q_{losses} - W_{electricity} = 0 \quad (19)$$

COST ESTIMATION METHODOLOGY

The capital and operating costs were estimated for the stack electroreactor process concept using the software Aspen Process Economic Analyzer (APEA) which, like Aspen Plus, is licensed by Aspen Technology. APEA was linked to Aspen Plus to estimate costs by utilizing the output results of the Aspen Plus simulations. Table 2 summarizes the assumptions as well as the prices of raw materials and utilities specified in APEA.

The capital investment is comprised of installed equipment costs, indirect costs (e.g. contingency), tax and working capital [26]. The capital investment required to establish the project is considered to be borrowed and repaid over the lifetime of the project (20 years) at a loan interest rate of 10% per annum. To estimate the fuel production costs of the electroreactor system, the annual amount required to pay back the loan on capital needs to be determined first:

$$A = TCI \cdot \frac{r \cdot (1+r)^N}{(1+r)^N - 1} \quad (20)$$

where *A* is the annuity of the capital investment, *TCI* the total capital investment as calculated in APEA, *r* the interest rate and *N* the lifetime of the project.

The total annual costs consist of capital annuities as well as operating costs: raw material, utilities, labor, and maintenance costs. The fuel production costs are calculated by dividing the total annual costs by the amount of chemical (CH_2O_2) produced in a year. The price inflation of equipment and raw materials is not considered. Also, government subsidies, CO_2 credits and by-product revenues are excluded from the economic analysis.

Table 2. Economic inputs to Aspen Process Economic Analyzer (APEA)

General economic parameters:	
Base year	2017
Plant life	20 years
Plant annual operating hours	8000
Loan interest rate	10%
Tax	40%[a]
Contingency	18%[a]
Working capital	5% of *TCI*[a]
Raw material prices:	
Nafion™ membrane N117	$221 per m^2 [27]
H_2S	$25 per kg[28]
Catalyst ZnTe	$150 per kg[29 b]
Catalyst SnO_2	$150 per kg[30 b]
Silica	$4.5 per kg[31]
Utility prices :	
Electricity	$0.007 per kW h [32 b]
Water	$0.66 per m^3 [33 b]

[a] APEA default values (country base: US). [b] Average sale price. Electricity price for small US industrial consumer.[32]

MODEL SIMULATION RESULTS

As stated previously, we modeled our system based on the 17 kW fuel cell stack, to complete our simulation. The calculated power requirement simulated for ten stacked cells was 17.2 kW which closely matched the system power specification for our 10-stacked cells. With inputted voltage '*EMF'* of 1.25 V, the calculated cell potential '*VCELL*' as given by Eqn. 15 was 1.238 V. This is quite a close value and shows the effectiveness of the *design spec* block used in the Aspen Plus simulation. The theoretical voltage given by the cell reaction chemistry for CH_2O_2 formation is 0.24 V. The ohmic overvoltage dominated the overvoltage with a value of 0.713 V while the cathodic and Nernst overvoltages were 0.319 and -0.034 V respectively. The negative Nernst value suggests negligible mass transport resistances and accounts for the high values of feed and product flow streams.

Table 3. Parameters and properties for the PEMEC model simulation showing stream cathode (SC) and stream anode (SA).

Stream No.	Temper-ature (K)	Pressure (bar)	Flow rates (kmol h^{-1})	Compositions									
				H_2S	CO_2	H_2	S	CH_2O_2	CO	H_2O	N	O_2	CH_4
SC2	540	9	967.5	-	921.4	-	-	-	2.6E-4	0.67	40.5	2.3	-
SA2	731	9	1138.2	1024.4	-	-	-	-	-	113.8	-	-	-
SC3	516	3	1061.7	-	921.4	-	-	-	76.3	3.3	50	2.3	8.5
SA3	682	3	1256.8	1024.4	-	-	113.8	-	-	118.6	-	-	-
SA5	393	3	2281.1	-	-	1024.4	1138.2	-	-	118.6	-	-	-
SC5	393	3.2	1571.1	-	-	-	-	538.1	406.9	515	50	1.3	61.2
SA9	393	3	118.6	-	-	-	113.8	-	-	4.7	-	-	-
SC9	151	2	94.3	-	-	-	-	-	76.3	-	9.5	-	8.5
SA8	120	3	1067.1	-	-	-	1024.4	-	-	42.7	-	-	-

For a 2e$^-$ transfer and 85% feed utilization, as shown in Table 3, Eqns. 3, 8, and 9 dominated since less energy was required for their formation compared to other products. During the simulation, all the possible reaction Eqns. 1-10 were entered in the simulator and the results are shown in Table 3. However, other variables such as temperature, and pressure also contributed to the faradaic yield obtained for CH_2O_2 as discussed in the sensitivity analysis section. The gross efficiency based on the power usage and the heating value of hydrogen fuel is 24% while the faradaic efficiency calculated from the conversion of feed to product is 95% given the overall efficiency of the system to be 23%. However, if the faradaic efficiency is based on CH_2O_2 formed, this value will reduce to 52%. In practice, this can be optimized to a higher value by use of catalytic electrode interfaces which were not considered in this model since AspenPlus^{TM} presently cannot be simulated for actual catalysts.

Table 4 is the result of energy simulation in the system. The energy balance is in agreement with the design parameters and the assumption of some heat losses in the system. This also is a validation of Eqn. 16 which gives a direct relationship between power and temperature.

Table 4. Energy balance for the stacked cells.

Stream No.	Heat values (kW)
QH2	1510.5
QH3	4224.07
QH4	5734.48
QH4 - (QH2+QH3)	0.09

ASPENPLUS^{TM} SENSITIVITY ANALYSIS

The developed model was run using a stream of CO_2 contained in a flue gas from coal-fired power plant and a stream of unmixed H_2S with some water vapor content. The result of the sensitivity analysis carried out in Aspen Plus process model are discussed next. Figs. 2 and 3 show the effect of feed utilization on H_2S feed, products issuing from the cathode, and cell potential respectively. The high rate of electrode reactions depicted by the current density, 6.098 mA cm^{-2}, in Fig. 2 resulted in the high consumption of H_2 which lead to a gradual decrease in its flow rate. At 60% U_{FUEL} operational condition, a sudden jump in the CH_2O_2 production is evident from a zero value and continued to increase with fuel utilization. High feed utilization is not favorable for the formation of other products specified in the electro-reactor. The cell potential virtually was constant with a value of 1.09 V up to 60% feed utilization after which a sudden rise in cell potential to a value of 1.238 V was experienced as shown in Fig.3. This sudden jump in the cell potential is attributed to increase in the cell electrode kinetics as a result of higher U_{FUEL} which, led to increase in the value of overpotential required (see Eqn.15). The H_2S feed flow rate continued to decline with feed utilization. There is no current literature reported experimental data available that utilizes CO_2 and H_2S simultaneously to produce CH_2O_2, however, we can site our preliminary experimental data as evidence. More also, Kortlever et al. has shown the feasibility of CO_2 conversion to CH_2O_2 [34]. The authors used $Pd_{70}Pt_{30}$/C catalyst and were able to obtain a faradaic efficiency of 88% toward formic acid after 1 h of electrolysis at a substantial lower overpotential −0.4 V vs RHE compared to our data, with an average current density of ~5 mA cm^{-2}. As mentioned previously, electrochemical splitting of H_2S to liquid sulfur and hydrogen is also feasible [8]. It must be pointed out that sulfur poisoning of the electrode material was observed in the experiment, which resulted in delamination of the electrode after 2 h even though sulfur is a low viscous fluid at the operating condition. We were unable to simulate this in AspenPlus because of its limitations.

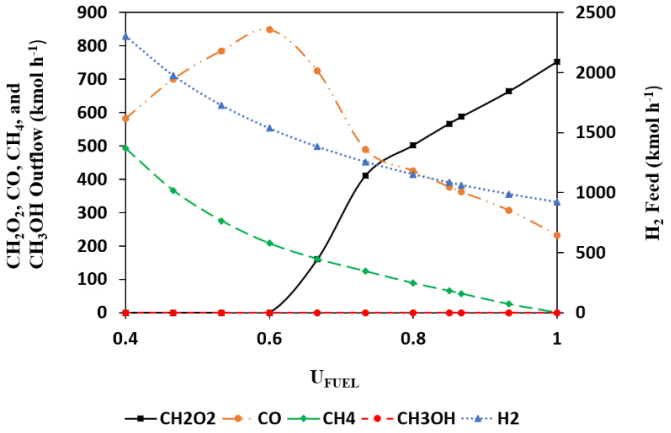

Figure. 2. Effects of U_{FUEL} on the product flow rates exiting cathode compartment, and the hydrogen equivalent flow rate entering the cathode compartment from the anode.

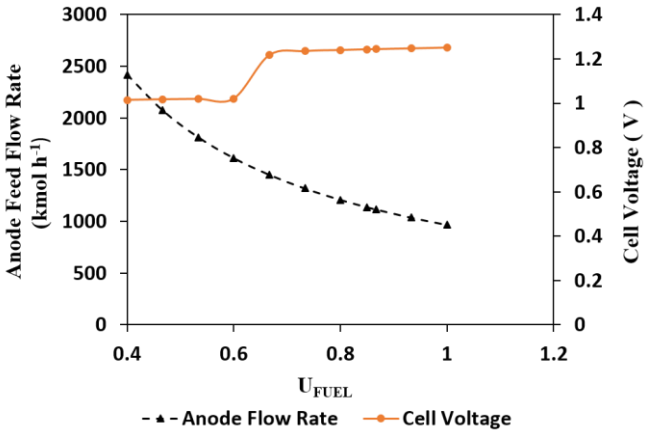

Figure. 3. Effects of U_{FUEL} on the cell voltage, and anode feed flow rate.

In Fig. 4, operating the PEMEC at a pressure of 3 bar is most favorable for CH_2O_2 and CH_4 formation than for CO but higher pressures above this value is most favorable for CO than it is for CH_2O_2. In fact, based on this simulation, the faradaic efficiency for CO is about 60% of the value obtained for CH_2O_2, 31% and 52% respectively at 3 bar. Based on our

cell configuration, the optimum pressure of 3 bar favors the electrode kinetics for the formation of CH_2O_2 and CH_4. The method of calculation of faradaic efficiency was discussed in the previous section. Pressure had no effect on CH_3OH formation and continued to maintain zero value in the product stream. Since the objective is to convert H_2S and CO_2 to CH_2O_2 operating the system at 3 bar will lead to a better yield. However, a pressure drop of 0.09 bar was needed to push the molten sulfur out of the anode compartment.

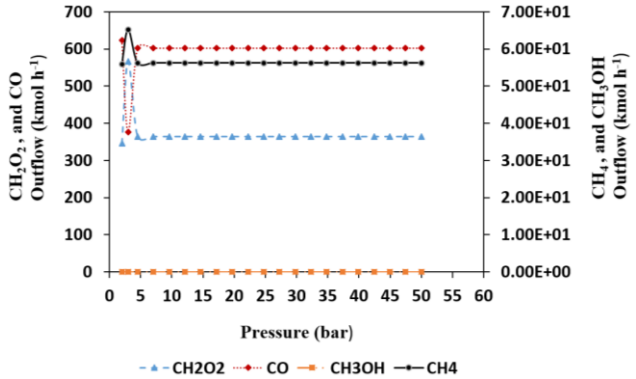

Figure. 4. Effects of cell pressure on the product flow rates exiting cathode compartment.

Fig. 5 shows the effect of temperature on the cell voltage, current density and required H_2S input for a PEMEC at a constant power output of 17.2 kW. If temperature is increased from 50 to 90°C, the cell potential increased slightly but experienced a jump at about 100°C and continued to increase because of more power input to the system. Although, one would expect an increase in the kinetics as a result of increase in temperature, however, this increase did not affect the fuel utilization and even though the flow rates of H_2 from H_2S splitting and flue gases continued to increase with temperature. A probable cause will be that at any given temperature the reactants were already fed in excess of their requirements an effect caused by the stoichiometric number associated with the feed flow rates.

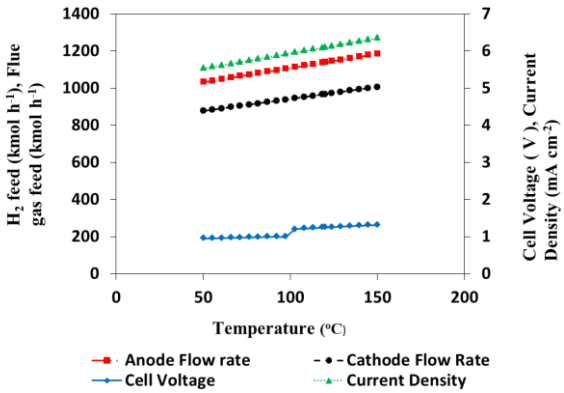

Figure. 5. Effects of operating temperature on the hydrogen equivalent flow rate, flue gas flow rate, cell voltage, and the current density.

Since there is a correlation between power and temperature (see Eq. 17), and power is directly proportional to current density and voltage, any increase in temperature would have a corresponding influence on the current density. Nevertheless, temperature has significant impact on the current density as a result of increase in the cells kinetics. Thus, both the gross efficiency based on the power usage and the faradaic efficiencies based on CH_2O_2 formation are expected to improve with temperature at temperatures at which sulfur is a low viscous fluid and can easily flow out of the PEMEC without hindrance.

ECONOMICS ANALYSIS

Table 5 shows the breakdown of capital costs for the electrochemical plant investment and the resulting total capital investment (TCI) for the electroreactor process designs. The calculated TCI is expressed in 2016 million $US $11.135 million.

The annual operating and maintenance (O&M) costs is $4.725 million. The operating costs include expenditure for materials (e.g., catalysts, H_2S), utilities (e.g., electricity), labor, maintenance and other costs (e.g., overheads, insurance). Annualized capital cost and electricity costs are the largest contributor to O&M costs.

Table 5. Economic Analysis of Hydrogen Sulfide + Carbon Dioxide Conversion

PLANT PARAMETERS	
COAL FIRED BOILER Plant Capacity (Gross MW)	500
On Line (Hours/year)	8000
Coal Consumption (Tons/day)	63
Coal sulfur content (%)	2.5
ELECTROCHEMICAL PLANT INVESTMENTS	
Apparatus to Remove Carbon Dioxide	$ 1,350,000
Electrolyzer	$ 6,460,000
Balance of Plant	$ 3,325,000
Total Electrochemical Plant Investments	$11,135,000
ANNUAL CAPITAL AND O&M COSTS	
Annualized Capital Costs	$ 1,500,000
Labor	$ 525,000
Catalysts, H_2S, water and other operating costs	$ 200,000
Electricity	$ 2,500,000
Total Annual Capital and O&M Costs	$ 4,725,000
FORMIC ACID PRODUCTION COSTS	
Costs to Produce 1 Ton of S + 125lb. of H_2	$ 215
Avoided Cost of Claus Process/Ton of S	$ 137
Net Production Cost of 1lb. of H_2	($ 0.63)
Net Production Cost of 1 lb. of CH_2O_2	($ 0.30)
MARKET PRICE OF sulfur ($/LB)	$ 3.75
MARKET PRICE OF CH_2O_2 ($/LB)	$ 0.03
Cost of electricity US$/kWh	($ 0.07)
GROSS PROFIT ($/LB.)	$2.78

The production costs per lb of CH_2O_2 are presented. The calculated production costs do not include tax, duties, producer and retailer profits, marketing expenditure and distribution costs. From these it is clear that the amount of CH_2O_2 produced (and thus conversion efficiencies) is a very important element of the production costs; thus, its effect was investigated in the sensitivity analysis.

The cost of $137/ton of sulfur for performing the Claus process exceeds the $87/ton [35] market value of the sulfur. The $50/ton difference is a penalty that operators currently pay to get rid of the hydrogen sulfide byproduct gas. This penalty would be avoided by using the electrolytic

process where the total value of the products (sulfur and CH_2O_2) exceeds the cost of the electrochemical processing. Formic acid costs will vary based on location and also by the quantity. The \$2.78/lb profit on the CH_2O_2 and sulfur increases the cost effectiveness of the electroreactor process. This is accomplished without claiming any economic credit for purifying the CO_2 in the acid gas to make it more suitable for conversion.

CONCLUSIONS

A model of the 17 kW PEMEC stack was developed using AspenPlus™. The objective of the study, which was to develop a computer simulation model of an electrolytic system capable of taking certain amount of CO_2 and H_2S content feed gases and transforming them to energy rich fuel, CH_2O_2, was achieved. The model uses existing AspenPlus™ unit operation blocks without extra external subroutine requirements thereby eliminating complexity and minimizing computational effort. The simulation result for the cell potential agreed well with the experimental observed value however, the current density deviates significantly. But with refined catalysts synthesis, this gap will reduce. The cell operated at a moderate optimum pressure of 3 bar and at 120°C, a temperature at which sulfur is a low viscous fluid and can flow out of the electrolytic cell without hindrance. At this pressure, the boiling point of water is elevated beyond 100°C and would keep the Nafion composite membrane which, served as the solid electrolyte hydrated. The economics of this process rely heavily on power and electrolyzer stacks. When dealing with electrolysis, optimization of these two parameters is needed. To perform this optimization, we utilized the best configuration used in our material balance analysis: current density of 6.098 mA cm^{-2} at a cell potential of -1.238 V were used.

The results indicate that there must be a balance between voltage and current density with respect to feed utilization and temperature should be operated at above 60% and above 100°C values respectively. Temperature has significant impact on the current density as a result of increase in the cells kinetics. Thus, system efficiencies are expected to improve with temperature. However, this increase must be limited to temperatures at which sulfur is a low viscous fluid between 120 – 135°C.

The simulation package may not be flexible with some parameters, for example, it was not possible to study the changes of feed utilization with respect to current density because the order of computation matters a lot using this model. But with advancement in AspenPlus™, a future version may be able to handle this present complexity easily.

ACKNOWLEDGEMENTS

Fund for this project was made available by FIT Start-up grant.

REFERENCES

[1] C. Song, A. M. Gaffney, K. Fujimoto, (Eds). *ACS*. (Washington DC, ACS Symp. Series) 2002, 809, 448.
[2] S. Pacala, R. Socolow, *Science*. 2004, 305, 968.
[3] M. I. Hoffert, *Science*. 2010, 329, 1292.
[4] S. J. Davis, K. Caldeira, H. D. Matthews, *Science*. 2010, 329, 1330.
[5] D. T. Whipple, P. J. A. Kenis, *J. Phys. Chem. Lett*. 2010, (1), 3451.
[6] H. R. Jhong, S. Ma, P. J. A. Kenis, *Current opinion in chemical engineering*. 2013.
[7] X. Xu, C. Song, R. Wincek, J. M. Andresen, B. G. Miller, A. W. Scaroni, *Fuel Chemistry* 2003, 48(1): 162.
[8] J. Mbah, B. Krakow, E. Stefanakos, J. Wolan, *J. Electrochem. Soc*. 2008, 155 (11): E166-E170.
[9] R. O'Hayre, S. Cha, W. Colella, F. Prinz, *Fuel cell fundamentals*, Wiley, third ed., New Jersey, 2016.
[10] W. Zhang, E. Croiset, P. L. Douglas, M. W. Fowler, E. Entchev, *Energy Conversion and Management*. 2005, (46), 181–196.
[11] N. O. Egiebor, J. Mbah, *Handbook of climate change, mitigation and Adaptation.* 2017, pp 2757-2774.
[12] X. Ren, T. D. Myles, K. N. Grew, W. K. S. Chiu, *J. Electrochem. Soc*. 2015, 162 (10): F1221-F1230.
[13] M. Jonson, G. D. Mahan, *Phys. Rev.* 1980, B 21 4223.
[14] D. Schweitzer, H. Pape, L. Chen, R. Kutscherauer, M. Walder, (*27th Annual IEEE Semiconductor Thermal Measurement and Management Symposium*). 2011, p. 222.
[15] T. Ho-Ming, L. Yi-Shao, C. P. Wong, *Springer Science & Business Media,* (Advanced Flip Chip Packaging). 2013, pp. 460–461. ISBN 978-1-4419-5768-9.
[16] Y. Shabany, *Heat Transfer: Thermal management of electronics*, CRC Press, 2011, pp. 111–113, ISBN 978-1-4398-1468-0.
[17] M. Lenz, G. Striedl, U. Fröhler, *Thermal resistance, theory and practice,* Infineon Technologies AG, Munich, Germany, 2000.
[18] C. J. M. Lasance, A. Poppe, *Thermal Management for LED Applications*, Springer Science & Business Media, 2013, p. 247. ISBN 978-1-4614-5091-7.
[19] C. J. M. Lasance, *Ten Years of boundary-condition-independent compact thermal modeling of electronic parts: A Review*, Heat Transfer Engineering. 2008, 29 (2) 149.
[20] M.S. Eikeland, R.K. Thapa, B.M. Halvorsen, *Proceedings of the 56th SIMS*, 2015, October 07-09, Linköping, Sweden.
[21] W. Doherty, A. Reynolds, D. Kennedy, *ECS Transactions*, 2009, 25 (2): 1321-1330.
[22] S. P. Cadogan, G. C. Maitland, J. P. M. Trusler, J. Chem. Eng. Data, 2014, 59: 519−525.
[23] https://www.osti.gov/scitech/servlets/purl/775213
[24] J. Zhang, Z. Xie, J. Zhang, Y. Tang, C. Songa, T. Navessin, Z. Shi, D. Song, H. Wang, D. Wilkinson, Z. Liu, S. Holdcroft, *J. Power Sources*. 2006, (160) 872–891.
[25] Aspen Plus™ 11.1 (2016) Users Guide, Aspen Tech

Ltd, Cambridge MA, USA.
[26] Aspen Technology, Aspen Icarus Reference Guide – Icarus Evaluation Engine (IEE), Burlington, USA, 2016.
[27] http://www.nafionstore.com/store/products/60/Nafion-Membrane-N117.
[28] https://www.alibaba.com/product-detail/99-9-gas-hydrogen-sulfide- price_60657614261.html.
[29] https://www.alibaba.com/showroom/cdte.html.
[30] https://www.alibaba.com/showroom/price-tin-oxide.html.
[31] https://www.alibaba.com/showroom/silica-price-per-ton.html.
[32] https://www.eia.gov/electricity/monthly/epm_table_grapher.php?t=epmt_5_6_a.
[33] http://www.earth-policy.org/plan_b_updates/2007/update64.
[34] R. Kortlever, I. Peters, S. Koper, M. T. M. Koper, *ACS Catal.* 2015, *5* (7): 3916–3923.
[35] http://marketrealist.com/2017/02/mosaics-raw-material-costs-4q16-compared-markets/.